

## Photocatalytic efficiency of $\text{CuFe}_2\text{O}_4$ by supporting on clinoptilolite in the decolorization of acid red 206 aqueous solutions

Azar Bagheri Ghomi\*, Vahid Ashayeri

Department of Chemistry, Center Tehran Branch, Islamic Azad University, Tehran, Iran.

Received 13 May 2012; received in revised form 15 October 2012; accepted 17 October 2012

### ABSTRACT

In this paper  $\text{CuFe}_2\text{O}_4$  nanocrystalline powders were prepared. Also, the supported Cu ferrite was obtained by impregnation of the supports with Cu and Fe nitrates solutions, for calcination temperature 450 °C. The samples were characterized by X-ray powder diffraction (XRD) and Fourier transform-infrared spectroscopy (FT-IR). Photocatalytic degradation of acid red 206 in water was studied.  $\text{CuFe}_2\text{O}_4$  was supported on Clinoptilolite using solid-state dispersion (SSD) method. The results show that the  $\text{CuFe}_2\text{O}_4/\text{zeolite}$  is an active photocatalyst. The maximum effect of photodegradation was observed at 10 wt. %  $\text{CuFe}_2\text{O}_4$ , 90 %wt. Clinoptilolite. A first order reaction with  $k = 0.123 \text{ min}^{-1}$  was observed. The effects of some parameters such as pH, amount of photocatalyst, initial concentration of dye were examined.

**Keywords:** Photodegradation, Photocatalysts,  $\text{CuFe}_2\text{O}_4/\text{Zeolites}$ , Acid Red 206, Clinoptilolite.

### 1. Introduction

Dye, a constituent that is widely used in textile, paper, plastic, food and cosmetic industries is an easily recognized pollutant. Many dyes are toxic to some microorganisms, and may cause direct destruction or inhibition of their catalytic capabilities [1]. Its presence, even in very low concentration, is highly visible and will affect aquatic life as well as food web. The conventional methods of color removal from industrial effluents include ion exchange, activated carbon adsorption, membrane technology and coagulation [2]. Catalytic oxidation has been extensively studied for the destruction of refractory and hazardous pollutants found in groundwater, surface water, and industrial wastewater [3-5]. Currently, these oxidation technologies are usually used directly in raw water matrix for decomposing organic compounds [6,7]. Copper ferrite ( $\text{CuFe}_2\text{O}_4$ ) is one of the important ferrites [8] and most effective photocatalysts.

The magnetic behavior of  $\text{CuFe}_2\text{O}_4$  has been drawn much interest and has been a subject of intensive studies [9,10]. Magnetic separation is considered as a high speed and effective technique for separating magnetic particles. Thus, if the powder adsorbent/ catalyst are magnetic, it could be recovered conveniently by magnetic separation technology.

It is known that copper ferrite is magnetic material. It has been used for many applications in biochemistry, microbiology, cell biology, analytical chemistry, mining ores, environmental technology and wastewater treatment [11,12]. However, the need to filter  $\text{CuFe}_2\text{O}_4$  after reaction makes such a process troublesome and costly. Thus, in order to solve this problem, many researchers have examined methods for fixing  $\text{CuFe}_2\text{O}_4$  on supporting materials including zeolite.

In this work, we reported the synthesis and characterization of  $\text{CuFe}_2\text{O}_4$  nanoparticles. The  $\text{CuFe}_2\text{O}_4$  was supported on zeolite without losing photoefficiency and affecting the adsorption properties of zeolite.  $\text{CuFe}_2\text{O}_4$  was used for degradation of aqueous Acid Red 206. The Chemical Oxygen Demand (COD) test is done.

### 2. Experimental

#### 2.1. Materials

All the compounds used were prepared from Merck Company and the raw zeolite material was an Iranian commercial Clinoptilolite (CP) (Afrand Tuska Company, Iran) from deposits in the region of Semnan. According to the supplier's specification, it contains about 90 wt.% CP (based on XRD internal standard quantitative analysis) and the Si/Al molar ratio is 5.78. The concentration of  $\text{Fe}_2\text{O}_3$ , MnO and  $\text{P}_2\text{O}_5$  impurities have been reported to be 1.30, 0.04 and 0.01 wt.%.

\* Corresponding author: E-mail: azar.bagheri@iauctb.ac.ir.  
Tel: +98 2188385777, Fax: +98 2188371939.

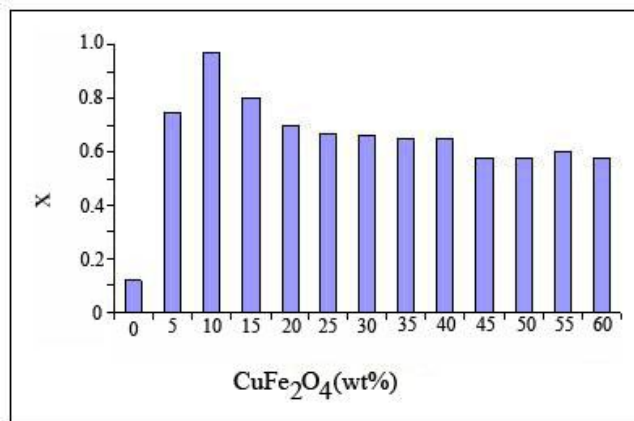


**Fig. 1.** Effect of composition of photocatalyst (wt.% CuFe<sub>2</sub>O<sub>4</sub> in mixture of CuFe<sub>2</sub>O<sub>4</sub> and CP) on photocatalytic degradation of AR206 after 120min.

In order to remove the impurities, the powdered Clinoptilolite was submitted to an acid treatment, using 1N HCl solutions and thermally treated in their sodium cation form at 673K during 4h. The azo dye, Acid Red 206, was obtained from the Kimiagostar Company (Iran) and used without further purification.

## 2.2. Apparatus

For the UV/photocatalyst process, irradiation was performed in a batch photoreactor of 2 liters in volume with four mercury lamps, Philips 8W (UV-C). A magnetic stirrer was used to ensure complete mixing in the tank (stirring speed = 250 rpm) and air was dispersed at a flow rate of 1 lit. min<sup>-1</sup> by using an air diffuser to supply oxygen for the enhancement of photo-oxidation. UV-Vis Spectrophotometer, (Shimadzu 2101) was employed for absorbance measurements using silica cells of path length 1 cm. XRD analysis of the samples was done using a D-500 diffractometer (Siemens). FTIR spectra were recorded on a Nicolet-Magna 550 equipment, with CsI optics.

## 2.3. Preparation of CuFe<sub>2</sub>O<sub>4</sub> and CuFe<sub>2</sub>O<sub>4</sub>-Supported CP Catalysts

For Preparation of CuFe<sub>2</sub>O<sub>4</sub>, 0.005 mol Cu(NO<sub>3</sub>)<sub>2</sub> and 0.01mol Fe(NO<sub>3</sub>)<sub>3</sub> were dissolved together in 50 ml distilled deionized water to get a mixed solution. The mixed solution was subsequently added into 100 ml 0.3M citric acid solution and produced a transparent mixed sol. During this mixing procedure, the temperature was controlled at around 80°C by using a water bath. Then the temperature was further kept at 80°C until a transparent and viscous gel was obtained. The as-obtained gel was subsequently transferred into an oven and kept at 130°C for 3 h. The as-prepared precursors were then annealed at 450°C for 3 h with a heating rate of 10°C/min.

The solid state dispersion (SSD) method was used for preparing the zeolite-based photocatalyst. In this method, CuFe<sub>2</sub>O<sub>4</sub> was mixed with zeolite using ethanol as a solvent

using an agate pestle and mortar; the solvent was then removed by evaporation. Samples prepared by this method were dried at 110°C and calcined in air at 450°C for 5 h to obtain CuFe<sub>2</sub>O<sub>4</sub>-supported zeolite catalysts.

## 2.4. Degradation experiments

For the photodegradation of Acid Red 206, a solution containing a known concentration of dye and photocatalyst was prepared and was allowed to equilibrate for 30 min in the darkness. The suspension pH values were adjusted at the desired level using dilute NaOH and H<sub>2</sub>SO<sub>4</sub> (the pH values were measured with a Horiba D-14 pH meter). The photo degradation reaction took place under the radiation of a mercury lamp while agitation was maintained to keep the suspension homogeneous. The concentration of the samples was determined using a spectrophotometer (UV-Vis Spectrophotometer, Shimadzu 160A) at λ<sub>max</sub> = 513 nm. The samples were filtered before the UV-Vis spectroscopy to remove the photocatalyst. The degree of photodegradation (X) as a function of time is given by:

$$X = \frac{C_0 - C}{C_0}$$

Where C<sub>0</sub> and C are the concentration of dye at t = 0 and t, respectively.

### 2.4.1. Procedure of determination of Chemical Oxygen Demand (COD)

50 ml of sample was taken into a refluxing flask and several boiling stones were added. 0.4 g HgSO<sub>4</sub> was added to the solution. 5 ml of concentrated H<sub>2</sub>SO<sub>4</sub> was also added to the solution. Finally Potassium dichromate was added. Thorough mixing of the solution was ensured by swirling the flask in a water bath to recover any volatile substances that may have escaped from the liquid state. The flask was then attached to the condenser and further cooling was done. 20 ml of sulphuric acid was added to the solution in the flask continuing cooling and swirling to mix the solution. The solution was refluxed for 1 hour. The reflux flask was rinsed thrice, pouring the rinsing water to the Erlenmeyer flask. The solution was diluted to about 300 ml and about 8 drops of phenanthroline ferrous sulphate was added to the solution as an indicator. The solution was titrated against the Mohr's salt and the titer volume required for the color change from blue-green to reddish blue was noted.

## 3. Results and Discussion

CuFe<sub>2</sub>O<sub>4</sub> can be used in the form of a fine powder or crystals dispersed in wastewater treatment applications. The enhanced photocatalytic activity over the composite CuFe<sub>2</sub>O<sub>4</sub>+CP reflects the beneficial adsorption properties of CP. Experimental results show that about 10 wt % of CuFe<sub>2</sub>O<sub>4</sub> with respect to zeolite is the best condition to achieve the synergism between CuFe<sub>2</sub>O<sub>4</sub> and CP (Fig. 1).

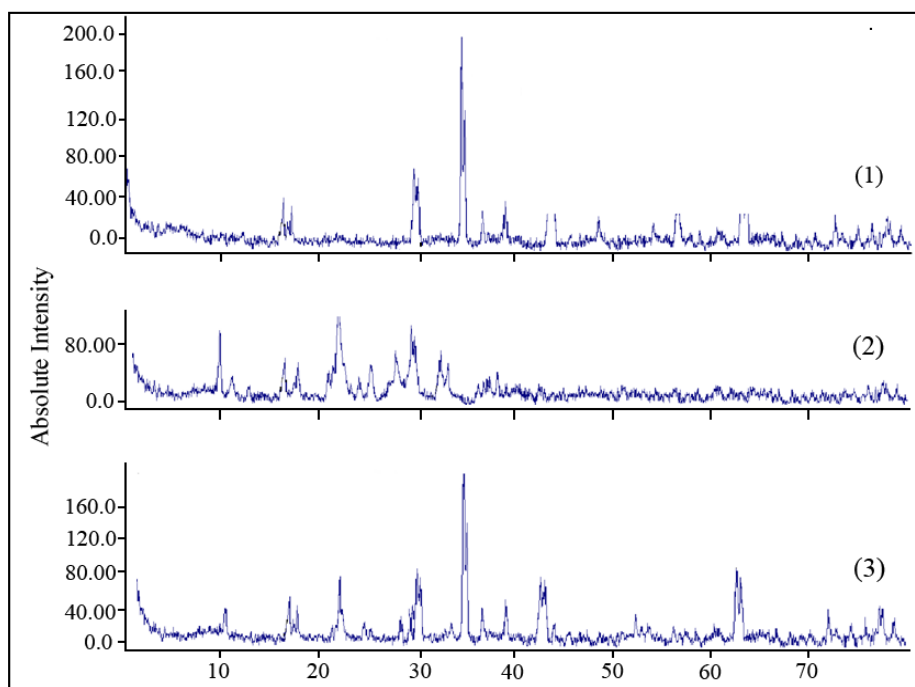


**Fig. 2.** XRD pattern of (1) raw  $\text{CuFe}_2\text{O}_4$  (2) CP (3) 10 wt.%  $\text{CuFe}_2\text{O}_4/\text{CP}$  prepared by the (SSD) method after calcination in air at  $450^\circ\text{C}$  for 5 h.

### 3.1. Characterization of Photocatalysts

The X-ray diffraction (XRD) pattern of copper ferrite sample is shown in Fig. 2. Sharp and well defined peaks are obtained. The presence of single phase  $\text{CuFe}_2\text{O}_4$  has been further confirmed by the absence of  $\text{CuO}$  and  $\text{Fe}_2\text{O}_3$  peaks. It is clear that the XRD patterns of  $\text{CuFe}_2\text{O}_4$ -zeolite consist with the raw zeolite very well as calcined at  $450^\circ\text{C}$  for 5 h, and no diffraction peaks corresponded to typical  $\text{CuFe}_2\text{O}_4$  can be observed and similar results have also been reported by other researchers. It implies that the frame structure of zeolite after  $\text{CuFe}_2\text{O}_4$  loading has not been destroyed.

The morphological feature of sample is shown in Fig. 3. The average particle size of the powder is in the range of about 100 nm.

The infrared analysis (Fig. 4) confirms that the  $\text{CuFe}_2\text{O}_4$  particles combine with the active sites of natural zeolite, Clinoptilolite, and Ti-O-Al and Ti-O-Si which make the load of  $\text{CuFe}_2\text{O}_4$ . Region of the spectrum, centered at  $3436\text{ cm}^{-1}$ , resulting from  $-\text{OH}$  stretching, is associated to the vibration of water molecules coordinated to zeolite structure. The absorptions associated to Fe/Cu complex with citrate, formed on the support surface and cavities, can be observed in the middle region of the spectrum. The frequencies around  $1383$  and  $1438\text{ cm}^{-1}$ , assignable to the functional groups present in the Fe/2Cu complex, as well as a band due to the free ligand centered in  $\sim 1631\text{ cm}^{-1}$ , are noticeable. It can be observed the most intense band of the spectrum, splitted in  $982$  and  $889\text{ cm}^{-1}$ , due to the stretching of Al-O-Si bonds of the tetrahedral building units forming the structure. The stretching vibration of O-H, mostly

corresponding to the surface  $-\text{OH}$ , shows a little weaker after  $\text{CuFe}_2\text{O}_4$  loading, indicating that a certain amount of  $-\text{OH}$  has been demolished by the load of  $\text{CuFe}_2\text{O}_4$ .

The existence of intense bands below  $600\text{ cm}^{-1}$ , corresponding to deformational modes of the condensed polyhedra  $\text{AlO}_4$  and  $\text{SiO}_4$ , forming the zeolitic lattice, restrain the detection of the bands associated to spinel mixed oxides that absorb in the same spectral region.

The surface area of the CP ( $480\text{ m}^2\text{g}^{-1}$ ) decreased in general on supporting  $\text{CuFe}_2\text{O}_4$  (BET surface area of  $\text{CuFe}_2\text{O}_4/\text{CP}$  with different  $\text{CuFe}_2\text{O}_4$  wt. is between  $290\text{--}374\text{ m}^2\text{g}^{-1}$ . BET surface area, confirmed catalytic activity.

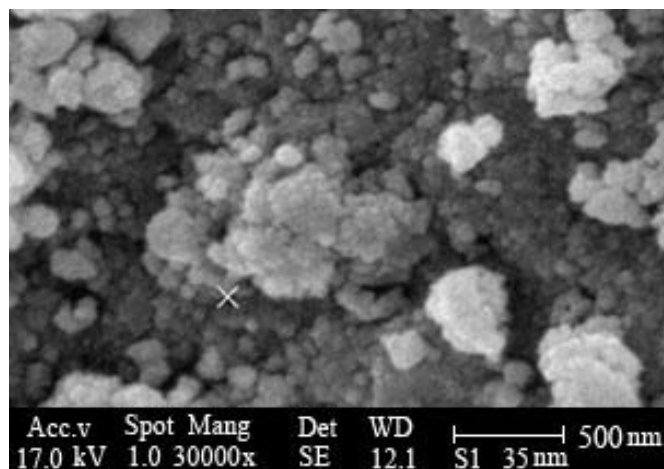


**Fig. 3.** SEM image of  $\text{CuFe}_2\text{O}_4$ .

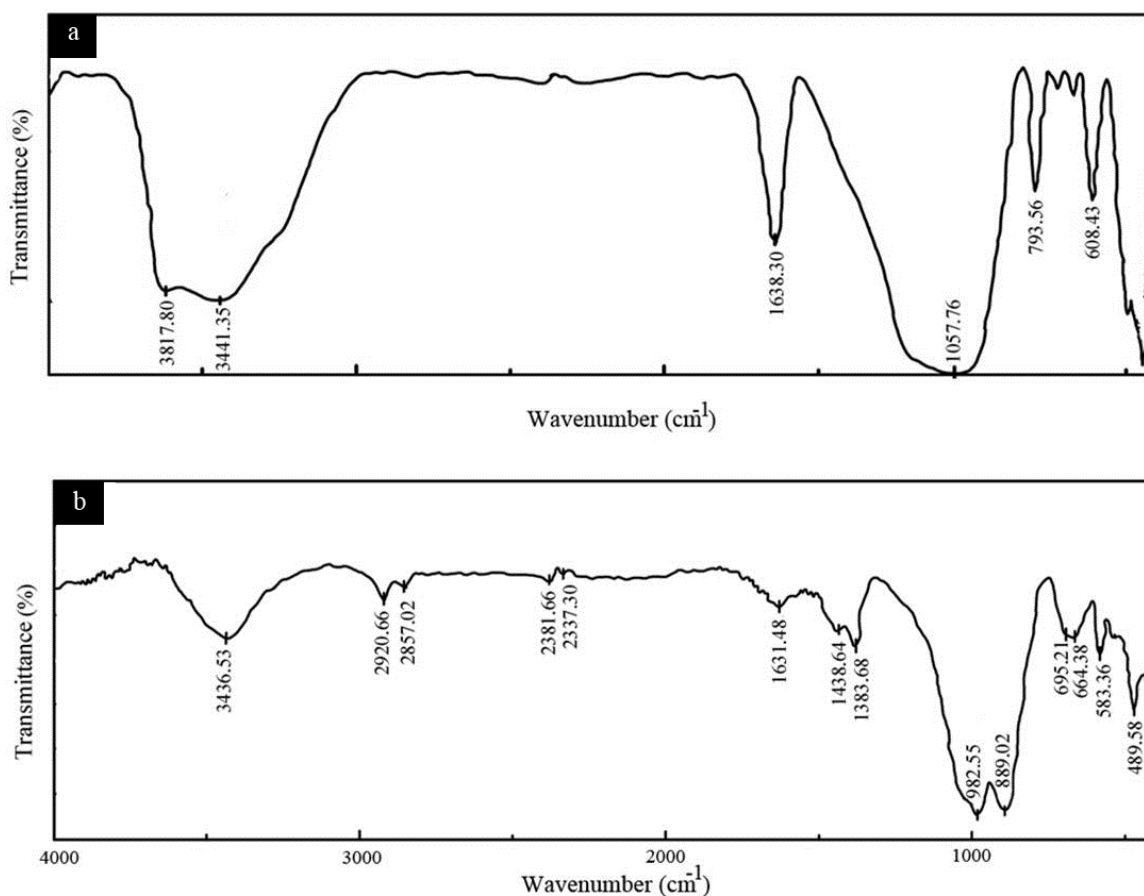


Fig. 4. (a) IR spectra of raw CP (b) CuFe<sub>2</sub>O<sub>4</sub>.

### 3.2. UV-Vis Spectra

The absorbance of Acid Red 206 solutions during the photocatalytic process at initial and after 2 h irradiation time verses  $\lambda$  are shown in Fig. 5. The decrease of absorption peaks of Acid Red 206 at  $\lambda_{\text{max}} = 513 \text{ nm}$  in this Figure indicates a rapid degradation of the azo dye. Complete discoloration of dye was observed after 3 h under optimum conditions.

### 3.3. Effect of Catalyst Concentration

The photodegradation efficiency increases with an increase in the amount of photocatalyst, up to a value of 80 ppm and then decreases when the catalyst concentration is increased. This trend can be explained by the fact that when all dye molecules are adsorbed on the photocatalyst, the addition of higher quantities of photocatalyst would have no effect on the degradation efficiency. Another reason for this is supposedly an increased opacity of the suspension, brought about as a result of an excess of photocatalyst particles [13]. To comment on this result, we propose that the  $\cdot\text{OH}$  (hydroxyl radicals), on the surface of CuFe<sub>2</sub>O<sub>4</sub>, are easily transferred on to the surface of zeolite. That means the organic pollutants, which have already been adsorbed on the non photoactive zeolite, have chances to be degraded due to

the appearance of  $\cdot\text{OH}$ , resulting in the enhancement of the photodegradation performance of CuFe<sub>2</sub>O<sub>4</sub>-zeolite.

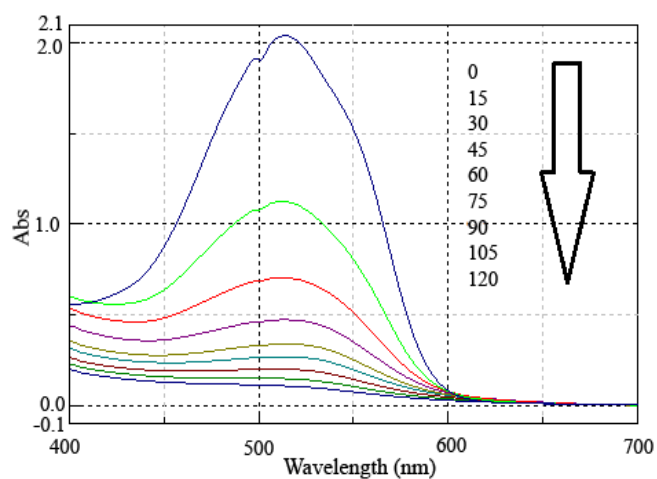


Fig. 5. UV-Vis spectra of AR206 (90 ppm) in aqueous photocatalyst dispersion with concentration of 60 ppm, irradiated with a mercury lamp light at pH = 4, T = 298 K, at: t = 0, 15, 30, 45, 60, 75, 90, 105, 120 min.

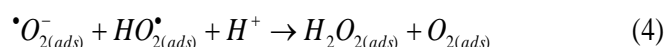
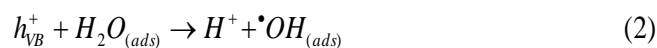
### 3.4. Effect of Initial AR206 Concentration

The effect of initial concentration of AR206 on photodegradation efficiency is studied. The photodegradation conversion of AR206 decreases with an increase in the initial concentration of AR206. The presumed reason is that when the initial concentration of dye is increased, more and more dye molecules are adsorbed on the surface of the photocatalyst. The large amount of adsorbed dye is thought to have an inhibitive effect on the reaction of dye molecules with photo generated sites or hydroxyl radicals, which is due to the lack of any direct contact between them. Once the concentration of dye is increased, it also causes the dye molecules to adsorb light and the photons never reach the photocatalyst surface, thus the photodegradation efficiency decreases.

### 3.5. Effect of pH

pH is one of the main factors influencing the rate of degradation of some organic compounds in the photocatalytic process [14,15]. It is also an important operational variable in actual wastewater treatment. The photodegradation of AR206 at different pH from 4 to 10 were studied. Many experiments were done for determination of optimum pH in according Taguchi experiments designs (Table 1) and the best results obtained in acidic solution (pH = 4) (Fig. 6).

The  $\text{CuFe}_2\text{O}_4$  surface is presumably positively charged in acidic solution and negatively charged in alkaline solution [16,17]. For the above reasons, for dyes that have a sulfuric group in their structure, which is negatively charged, the acidic solution favors adsorption of dye onto the photocatalyst surface, thus the photodegradation efficiency increases. There is also the photocatalytic degradation of AR206 in acidic solutions, which is probably due to the formation of  $\cdot\text{OH}$  as it can be inferred from the reactions (1-4) [18].



The fading of the solution was associated with cleavage of azo linkage in dye molecule. Azo dye are characterized by nitrogen to nitrogen double bonds that usually attached to two radicals of which at least one but usually both are aromatic groups. The cleavage of  $-\text{N}=\text{N}-$  bonds leads to the decolorization of dyes, what was observed in the discussed experiment. It can be observed that during irradiation not only a rapid decolorization of the dye, but also significant degradation of the aromatic structure proceeds. This could suggest that the dye was almost completely decomposed into  $\text{CO}_2$ ,  $\text{H}_2\text{O}$  and inorganic species ( $\text{SO}_4^{2-}$  and  $\text{NO}_3^-$ ).

**Table 1.** The brief of done experiments in photocatalytic analysis of AR 206.

Experiment number	Dye (ppm)	Cat (ppm)	pH
1	30	20	4
2	60	40	4
3	90	60	4
4	120	80	4
5	90	20	6
6	120	40	6
7	30	60	6
8	60	80	6
9	120	20	8
10	90	40	8
11	60	60	8
12	30	80	8
13	60	20	10
14	30	20	10
15	120	60	10
16	90	80	10

### 3.6. Kinetics of Photocatalytic Degradation of AR206

Several experimental results indicated that the degradation rates of photocatalytic oxidation of various dyes over illuminated  $\text{CuFe}_2\text{O}_4$  fitted by the first-order kinetic model [19-25]. The linear plot suggests that the photodegradation reaction approximately follows the pseudo-first order kinetics with rate coefficient  $K = 0.123 \text{ min}^{-1}$ .

### 3.7. Chemical Oxygen Demand (COD)

Sanitary landfills are the primary method currently used for municipal solid waste disposal in many countries, and leachate generated from landfills is a high-strength

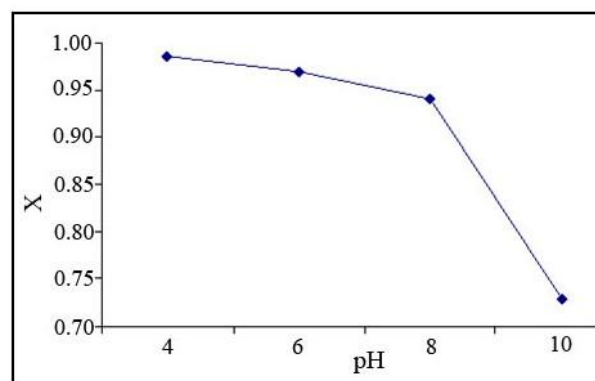


**Fig. 6.** Effect of pH on photodegradation efficiency of AR206 in 298K. Irradiation time = 1.0 h.

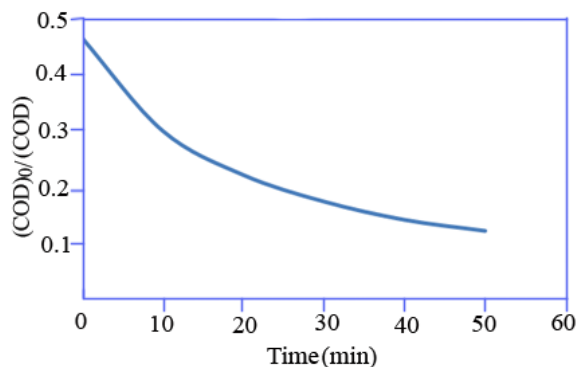


Fig. 7. Plot of COD changes in photocatalyst analysis of AR206.

wastewater exhibiting acute and chronic toxicity. The Chemical Oxygen Demand (COD) test is used widely to estimate the amount of organic matter in wastewater. The impact of an effluent or waste water discharge on the receiving water is predicted by its oxygen demand. As seen in Fig. 7, it observes that the dye remove in presence of UV-Vis irradiation.

### 3.8. Reuseability of photocatalyst

It is important to use the catalysts in which active species loaded on zeolite to be reusable without significant loss of activity and with minimal need for regeneration. In order to investigate the reusability of the catalyst, experiments were performed under similar conditions for three cycles. It was concluded that after 3 cycle 70% of efficiency was remained.

## 4. Conclusions

- 1- The SSD method is an effective method for supporting  $\text{CuFe}_2\text{O}_4$  on CP.
- 2- The photodegradation conversion of AR206 decrease with an increase in the initial concentration of AR206.
- 3- pH is one of the main factors and the optimum pH was obtained about 4.
- 4- Kinetics of photocatalytic degradation of AR206 is pseudo-first order with  $K = 0.123 \text{ min}^{-1} \cdot \text{s}$ .

## References

- [1] A.K. Vinodgopal, I. Bedja, S. Hotchandani, P.V. Kamat, *Langmuir* 10 (1994) 1767-1771.
- [2] K. Tanaka, K. Padermpole, T. Hisanaga, *Wat. Res.* 34 (2000) 320-333.
- [3] A.G. Gullis, I.T. Canhan, P.D.J. Calcott, *J. Appl. Phys.* 82 (1997) 909-965.
- [4] G. Bomghil, A. Halimaouri, R. Herimo, *Fppl. Surf. Sci.* 41 (1989) 600-604.
- [5] L. Lucarelli, V. Nadtochenko, J. Kiwi, *Langmuir* 16 (2000) 1102-1105.
- [6] W.P. Kwan, B.M. Voelker, *Environ. Sci. Technol.* 37 (2003) 1150-1158.
- [7] L. Oliviero, J. Barbier Jr., D. Duprez, *Appl. Catal. B* 40 (2003) 163-184.
- [8] J. Bandara, J.A. Mielczarski, J. Kiwi, *Langmuir* 15 (1999) 7680-7689.
- [9] J.Z. Jiang, G.F. Goya, H.R. Rechenberg, *J. Phys. Condens. Mater.* 11 (1999) 4063-4078.
- [10] A.F.M. van Velsen, G. van der Vos, *Water Sci. Technol.* 24 (10) (1991) 195-203.
- [11] A.D. Ebner, J.A. Ritter, H.J. Ploehn, J.D. Navratil, *Sep. Sci. Technol.* 34 (1999) 1277-1300.
- [12] P.B. Pandya, H.H. Joshi, R.G. Kulkarni, *J. Mater. Sci. Lett.* 10 (1991) 473-474.
- [13] R. W. Matthews, *Solar Energy* 38 (1987) 405-413.
- [14] K. Hofstandler, K. Kikkawa, R. Bauer, C. Novalic, G. Heisier, *Environ. Sci. Technol.* 28 (1994) 670-674.
- [15] M. Anpo, H. Nakaya, S. Kodama, Y. Kubokawal, K. Domen, T. Onishi, *J. Phys. Chem.* 90 (1986) 1630-1633.
- [16] S. Sato, *Langmuir* 4 (1988) 1150-1156.
- [17] H. Yoneyama, S. Hag, S. Yamanaka, *J. Phys. Chem.* 93 (1989) 4833-4837.
- [18] Y.I. Kim, S.W. Keller, J.S. Krueger, E. H. Yonemoto, G.B. Saupé, T. E. Mallouk, *J. Phys. Chem. B* 101 (1997) 2491-2500.
- [19] M. Saquib, M. Muneer, *Dyes Pigments* 56 (2003) 37-49.
- [20] A.L. Linsebigler, L. Guangquan, J. T. Yates, *Chem. Rev.* 95 (1995) 735-758.
- [21] V. Augugliaro, C. Baiocchi, A. Bianco-Prevot, E. Garcia-Lopez, V. Loddo, S. Malato, G. Marci, L. Palmisano, M. Pazzi, E. Pramauro, *Chemosphere* 49 (2002) 1223-1230.
- [22] M. Styliidi, D.I. Kondarides, X. E. Verykios, *Appl. Catal. B: Environ.* 40 (2003) 271-286.
- [23] G.A. Epling, C. Lin, *Chemosphere* 46 (2002) 561-570.
- [24] Z. Shourong, H. Qingguo, Z. Jun, W. Bingkun, *J. Photochem. Photobiol. A Chem.* 108 (1997) 235-238.
- [25] M.S.T. Conçaves, A.M.F. Oliveira-Campos, M.M.S. Pinto, P.M.S. Plasencia, M.J.R.P. Queiroz, *Chemosphere* 39 (1999) 781-786.